Applied Catalysis B: Environmental 160–161 (2014) 122–128

Contents lists available at ScienceDirect

Applied Catalysis B: Environmental

journal homepage: www.elsevier.com/locate/apcatb

# Esterification of a waste produced from the palm oil industry over 12-tungstophosforic acid supported on kaolin waste and mesoporous materials

Luiza H.O. Pires[a,*], Alex N. de Oliveira[a], Ozéias V. Monteiro Jr.[a], Rômulo S. Angélica[b], Carlos E.F. da Costa[a], José R. Zamian[a], Luís A.S. do Nascimento[a], Geraldo N. Rocha Filho[a]

[a] Laboratório de Catálise e Oleoquímica, Universidade Federal do Pará, Rua Augusto Corrêa, Guamá, CEP: 66075-110, Belém, Pará, Brasil
[b] Laboratório de Difração de Raios-X, Universidade Federal do Pará, Rua Augusto Corrêa, Guamá, CEP: 66075-110, Belém, Pará, Brasil

ARTICLE INFO

*Article history:*
Received 16 February 2014
Received in revised form 4 April 2014
Accepted 22 April 2014
Available online 2 May 2014

*Keywords:*
Supported heteropolyacid
Kaolin waste
Mesoporous materials
Esterification

ABSTRACT

In this work, kaolin waste, MCM-41, MCM-48, and SBA-15 were impregnated with $H_3PW_{12}O_{40}$ (HPW). The obtained solid acid catalysts were characterized by various techniques, such as XRF, XRD, FTIR and $N_2$ adsorption. The surface acidities were measured by acid–base titration of KOH. The catalytic activities of the catalysts in the esterification reaction of a waste produced during the deodorization processes of palm oil (DDPO) were studied. The results revealed that the materials have great potential in promoting heterogeneous acid-catalyzed organic transformations.



## 1. Introduction

Biodiesel is a renewable, biodegradable, eco-friendly, and non-toxic fuel that consists of alkyl esters produced by either the transesterification of triglycerides or the esterification of fatty acids with short-chain alcohols and a catalyst [1,2].

The homogeneous base-catalyzed transesterification of vegetable oils with methanol is currently the most used commercial technology for biodiesel production. Although effective, this route commonly leads to undesired side reactions, such as saponification, which is common in raw material with a large quantity of free fatty acids (FFA) [3]. This way, the implementation of an effective separation and product purification protocol, increasing the production costs.

When using feedstock with high amounts of FFA, acid-catalyzed esterification is more efficient than base-catalyzed transesterification [4]. The esterification of long-chain carboxylic acids, such as oleic acid, has gained much attention in the context of biodiesel production because FFA may be present in different forms in vegetable oils as well as wastes and recycled lipid feedstock. The material obtained during the distillation process for the deodorization of palm oil (labeled DDPO) produced by the Companhia Refinadora da Amazônia, Agropalma S/A, is a good example of these type of wastes. The DDPO is an interesting alternative for biodiesel production because it consists of approximately 84% FFA [5].

Acid-catalyzed esterification is generally conducted in the liquid phase using mineral acid catalysts, such as $H_2SO_4$, HCl, HF, and $H_3PO_4$, which promote corrosion in the reactors and cause environmental problems [6]. The replacement of these mineral acid catalysts by heterogeneous acid catalysts would result in simplified product recovery and eliminate or reduce waste streams [7].

Solid acids, such as 12-tungstophosphoric acid (HPW), have attracted considerable attention because of their strong acidity, which presents possibilities for use as Brønsted acid catalysts. In the esterification of a long-chain carboxylic acid, these Brønsted acid sites reversibly protonate the carboxylic acid molecules, which are susceptible to attack by even a weak nucleophile, such as methanol or ethanol. A tetrahedral intermediate is formed, and it is protonated again. The loss of water from the tetrahedral intermediate pushes the reaction forward to the ester product [8].

The practical application of HPW is, however, limited due to its low surface area (1–5 $m^2/g$) and low thermal stability [9]. Researchers have demonstrated that a solution to these drawbacks is to support HPW over high surface area materials, such as MCM-41 [11], zirconia [12], SBA-15 [13], clay [27] and so on. In that

* Corresponding author. Tel.: +559181714947.
*E-mail addresses:* luizapires@ufpa.br (L.H.O. Pires), adrlui1@yahoo.com.br (L.A.S.d. Nascimento).

http://dx.doi.org/10.1016/j.apcatb.2014.04.039
0926-3373/

case, HPW clusters with diameters around 1.2 nm can be dispersed in the surface and/or introduced inside the pores of these solids, thus allowing for a significant increase in the surface area of the HPW with a possible increase in its thermal stability, in addition to creating Brønsted acid sites within the supports. So, the obtained materials can provide potential heterogeneous acid catalysts with high activity for a wide range of organic transformations, including esterification reactions.

Other inconvenience that have been reported that limits the application of HPW is its high solubility in polar solvents like water and ethanol, which leads to homogeneous catalyzed reactions [9,12]. Therefore, supporting HPW in an appropriated solid is a way to prevents leaching of the acid into the reagent solution maintaining the advantages of a heterogeneously catalyzed reaction.

Kaolin is a low cost clay material available worldwide. Its chemical formula is $Al_2Si_2O_5(OH)_4$, and its major mineral component is the double-layered clay kaolinite [14]. Kaolin has been used as in paper coating, paper filling, ceramics, and cement and as an adsorbent and a catalyst. The potential use of kaolin as adsorbent or catalyst resides in the possibility of modifying its surface to enhance the textural properties such surface area and pore volume [15].

The Amazon region, specifically the northeast of Pará (Brazil), possesses a vast reserve of high-whiteness kaolin, which is primarily used as a raw material for paper coating [16]. The kaolin processing industry produces more than 1 million tons of kaolin waste per year in the region. This waste is mainly composed of kaolinite and is derived from the centrifugation, magnetic separation, whitening and filtering processes. Kaolin is of inadequate size for paper coating [17]. Thus, a significant amount of kaolin waste is stored in waste disposal sites, causing a serious environmental problem in the region.

This study was performed in an attempt to use the widely available kaolin waste produced by kaolin industries as well as the waste produced during the distillation process for the deodorization of palm oil (DDPO). We report the esterification of DDPO with ethanol for ester production over a series of catalysts containing 20–40% of 12-tungstophosphoric acid supported on kaolin waste.

The reaction was also performed over MCM-41, MCM-48 and SBA-15 molecular sieves modified with 20% 12-tungstophosphoric acid. Ethanol was chosen because it is renewable, abundant and has low toxicity compared to methanol and other alcohols. The catalysts were characterized by various thermal and spectral techniques, such as XRD, FRX, FT-IR and $N_2$ fisisorption.

## 2. Materials and methods

### 2.1. Raw material and chemicals

The kaolin waste used in this study was provided by a kaolin industry located in the northeast of Pará, Brazil. The DDPO (viscosity at 60 °C = 12.296 $mm^2/s$; density at 60 °C = 0.862 g/mL; water content = 0.0%; oxidative stability >150 h; acidity index = 177.15 mg KOH/g) consisted of 84% FFA (where 42% palmitic, 41% oleic, 10% linoleic, 5% stearic, 1% lauric and 1% myristic acid), as well as 12 wt% triglycerides, diglycerides and monoglycerides, and 4 wt% unsaponifiable matter. It was obtained from the Companhia Refinadora da Amazônia, Agropalma S/A (Brazil).

The reagents were the following: ethanol (EtOH, Nuclear, 99.5%), 12-tungstophosphoric acid (HPW, Sigma-Aldrich, PA), tetraethyl orthosilicate (TEOS, Aldrich), ammonium hydroxide ($NH_4OH$, aqueous solution 25%, Aldrich), cetyltrimethylammonium bromide (CTAB, Aldrich), pluronic (P-123, Aldrich), hydrochloric acid (HCl, 37%, Vetec), and sodium hydroxide (NaOH, Vetec). All of the reagents were used as supplied.

### 2.2. Catalyst preparation

#### 2.2.1. Preparation of 20–40% HPW/MK700

First of all, kaolin waste was transformed into metakaolin by calcination at 700 °C for 2 h in a muffle furnace (Quimis, model 6318M24), under static air atmosphere. One gram of the metakaolin (labeled as MK700) was dispersed under vigorous stirring in an aqueous acid solution (HCl 0.1 mol/L) containing the desired amounts of HPW. The resulting slurry of HPW and MK700 was heated at 80 °C under constant stirring until the liquid was completely evaporated. The solid was pulverized and dried at 120 °C for 12 h and then calcined at 200 °C for 4 h at a heating rate of 10 °C/min. It is important to mention that HCl is eliminated (decomposed) during thermal treatment. The samples were labeled *x*-HPW/MK700, where *x* represents the respective HPW loadings supported on MK700, ranging from 20 to 40 wt %.

#### 2.2.2. Preparation of mesoporous materials

*2.2.2.1. MCM-41.* MCM-41 was synthesized according to the work of Cai et al. [18]. Two grams of CTAB, 100 mL of de-ionized water and 51.25 mL of $NH_4OH$ were mixed. The system was kept under stirring for 30 min, and 2.5 mL of TEOS was then added. The precipitated solid was stirred for 2 h, recovered by filtration and washed several times with de-ionized water. After drying overnight at room temperature, the organic surfactant was removed by calcination in air at 550 °C for 4 h (temperature ramp of 1 °C/min).

*2.2.2.2. MCM-48.* The MCM-48 was synthesized according to the procedure described by Schumacher et al. [19]. The CTAB was dissolved in deionized water, and TEOS and NaOH were added. The molar composition of the obtained gel was: $1TEOS/0.25Na_2O/0.65CTAB/0.62H_2O$. The solution was stirred for 1 h and heated at 110 °C for 3 days. According to the employed procedure, 3 days is the aging time required for the growth and development of the MCM-48 structure. The white powder obtained after this period of time was filtered, washed with water and calcined at 550 °C for 6 h to remove the template.

*2.2.2.3. SBA-15.* SBA-15 was synthesized using pluronic (P-123) as a structure-directing agent and TEOS as a silicon source [20]. A solution of -P123, $H_2O$ and HCl (2.0 M) was prepared with stirring at 35 °C. After complete dissolution, TEOS was added. The stirring was maintained at this temperature for 20 h. The obtained gel was crystallized at 80 °C for 24 h. The resulting material was filtered, washed, dried at room temperature, and lastly calcined at 500 °C for 6 h.

#### 2.2.3. Impregnation of mesoporous materials with HPW

The samples were prepared by impregnation in HCl (0.1 mol/L) as described in item 2.2.1. They were labeled as 25HPW/MCM41, 25HPW/MCM48 and 25HPW/SBA15.

### 2.3. Characterization of the catalysts

#### 2.3.1. X-ray fluorescence (XRF)

The chemical composition of the catalysts and the possible leaching of HPW from the supported catalysts post-esterification reaction were determined using a Shimadzu EDX-700 energy dispersive X-ray spectrometer with a rhodium X-ray source tube (40 kV).

#### 2.3.2. X-ray diffraction (XRD)

X-ray diffractograms were obtained using a PANalytical X'PERT PRO MPD (PW 3040/60) diffractometer using the powder method. Cu*K*α radiation (40 kV and 40 mA) was used. The $2\theta$ scanning speed was $0.02^\circ\ s^{-1}$.

**Table 1**
Chemical composition of kaolin waste (wt%).

| Sample | $SiO_2$ | $Al_2O_3$ | $Fe_2O_3$ | $TiO_2$ | Loss on ignition[a] |
|---|---|---|---|---|---|
| Theoretical kaolinite | 46.54 | 39.5 | – | – | 13.96 |
| Kaolin Waste | 35.59 | 36.34 | 3.25 | 2.57 | 22.24 |
| MK 700 | 44.80 | 48.00 | 4.06 | 3.12 | – |

[a] At 1000 ± 25 °C.

#### 2.3.3. Surface area measurements

Nitrogen adsorption/desorption isotherms were obtained at liquid nitrogen temperature using a Micromeritics TriStar II apparatus. Prior to adsorption measurements, the samples were degassed at 200 °C for 2 h. The surface area was determined according to the standard Brunauer–Emmett–Teller (BET) method. The pore diameter ($D_p$) and pore volume ($V_p$) were obtained by the Barret–Joyner–Halenda (BJH) method.

#### 2.3.4. Fourier transform infrared spectroscopy (FT-IR)

The infrared spectra were recorded in the 4000–500 $cm^{-1}$ spectral region using a Thermo IR100 spectrometer. Transmittance measurements were performed using KBr pellets containing 1 wt% of the sample to be analyzed.

#### 2.3.5. Surface acidity

The surface acidity was determined using acid–base titration [21]. One-half gram of the solid was dispersed in 50 mL of 0.1 M KCl. The dispersion was stirred for 20 min and titrated with 0.2 M KOH in the presence of phenolphthalein.

### 2.4. Reaction procedure

Before the experiments, all of the catalysts were subjected to a heating activation at 130 °C for 2 h in an oven. Preliminary reactions were performed in a PARR 4848 reactor. Standard experiments were conducted by combining 1 mol DDPO, 10 mol ethanol and 10 wt% catalyst. The temperature ranged from 70 to 200 °C. The reaction mixture was allowed to reach the desired temperature, and agitation was commenced at a known speed (500 rpm). After the completion of the reaction, the catalyst was separated by simple filtration. The ethanol and the water present in the filtrate were removed by evaporation. The conversion of fatty acid was estimated by measuring the acid value (A) of the product and calculated according to the report of Ozbay et al. [22], where an aqueous solution of 0.01 N NaOH was used as a titrant. The conversion ($C_{FFA}$) was determined according to the following equation:

$$C_{FFA}(\%) = \left(\frac{A_i - A_t}{A_i}\right) \times 100$$

The subscript "i" refers to the initial acidity level, and "t" refers to the acidity at a certain reaction time.

## 3. Results and discussion

### 3.1. XRF

The chemical composition of the kaolin waste, listed in Table 1, was consistent with previously published theoretical values for kaolin [16].

The actual HPW loadings of the samples MK700, MCM-41, MCM-48 and SBA-15 were also evaluated using tungsten oxide analysis by XRF. As the difference between nominal and the measured mass ratio was less than 5% in all cases, the solids were referred to by their nominal compositions.

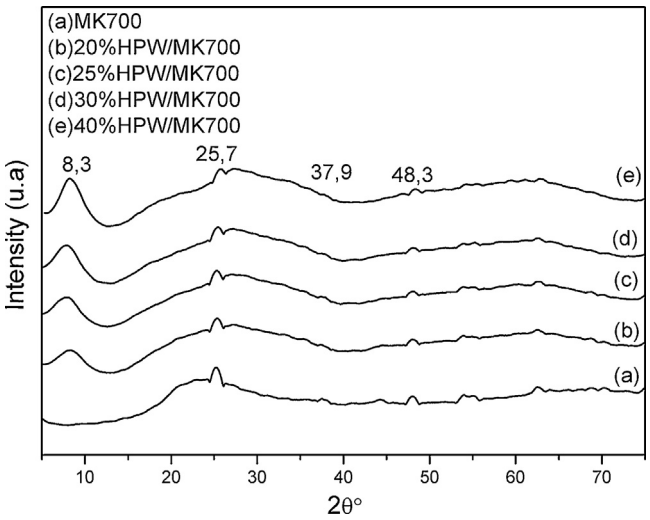


**Fig. 1.** XRD of MK700 and *x*%HPA/MK700.

### 3.2. XRD

Fig. 1 shows the XRD diffractograms of the MK700 and *x*%HPW/MK700 samples. All of the samples exhibited peaks at 2$\theta$ values of 25 °, 37 ° and 48 °, which were related to anatase ($TiO_2$), which is frequently found as an accessory mineral in kaolin from the Amazon region. The broad band between 15 ° < 2$\theta$ > 25 °, also found in these samples, was attributed to an amorphous phase of $SiO_2$ [23].

Fig. 2 shows the diffratogram for pure HPW. The reflections at around 2$\theta$ = 10, 20, 25 and 32° are characteristics of the crystalline phase of HPW [25,27]. The peak at 2$\theta$ = 8.3 ° which is present in the diffratogram patterns of *x*%HPW/MK700 samples (Fig. 1) can be related to different crystalline structures that HPW presents in the function of variable hydrated degrees of the heteropolyacid or addition of a base connected to $H^+$ in the secondary structure [29,30]. The absence of the other diffraction peaks due to the crystalline HPW phase in these solids suggests that HPW is probably well dispersed on the MK700 surface, forming very small crystallites that cannot be detected by XRD.

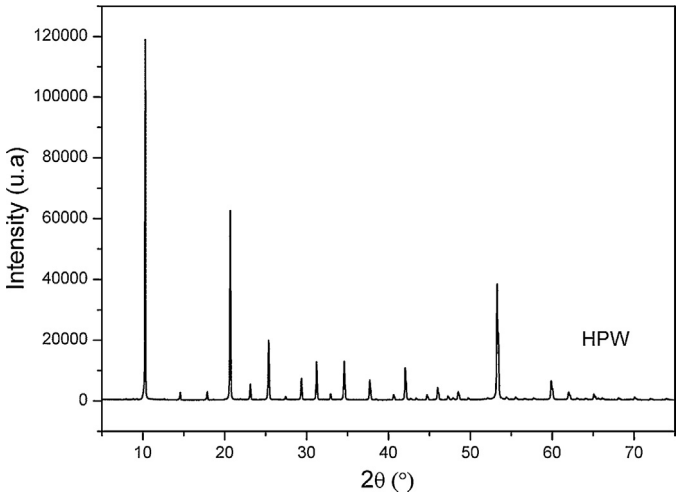


**Fig. 2.** XRD of pure HPA.

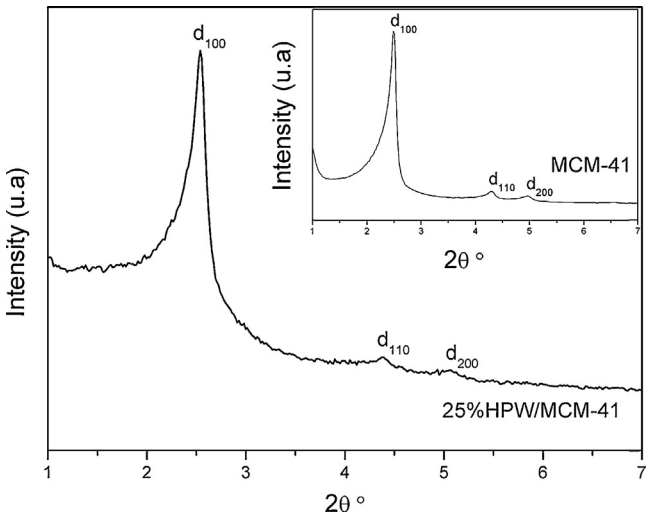


**Fig. 3.** XRD of MCM-41 and 25%HPW/MCM-41.

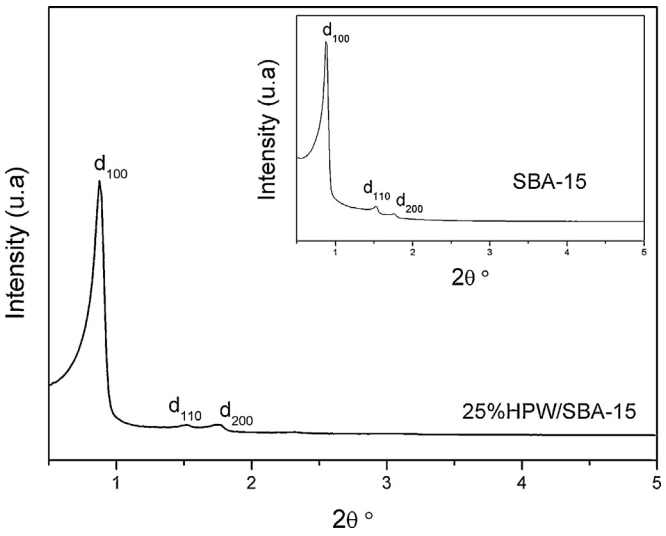


**Fig. 5.** XRD of SBA-15 and 25%HPW/SBA-1.

The diffractogram patterns of the mesoporous materials before and after the incorporation of different weight percentage loadings of HPW are shown in Figs. 3–5. Three characteristic peaks indexed as (1 0 0), (1 1 0) and (2 0 0) reflections were recognized in Fig. 3. They can be attributed to a well ordered hexagonal pore system typical of the MCM-41 structure. In the 25%HPW/MCM-41, these reflections become broader and weaker, suggesting that this sample possesses less ordered structure compared to MCM-41; however, the mesopore structure and the hexagonal ordering was retained after the introduction of HPW [11].

The cubic and hexagonal symmetries for MCM-48, 25%HPW/MCM-48, SBA-15 and 25%HPW/SBA-15 molecular sieves were also confirmed by the XRD reflections. Three peaks at (2 1 1), (2 2 0) and (3 3 2) related to the cubic phase (*Ia3d*) were observed for the MCM-48 sample (see Fig. 4). The disappearance of the (3 3 2) peak for the 25%HPW/MCM-48 sample suggested that this sample is less ordered compared to MCM-48 [19,24]. The XRD patterns of SBA-15 and 25%HPW/SBA-15 (Fig. 5) exhibited (1 0 0), (1 1 0), and (2 0 0) reflections of a 2D hexagonal structure [20,22]. These results indicated that the ordered hexagonal structure of SBA-15 remains intact after the deposition of HPW.

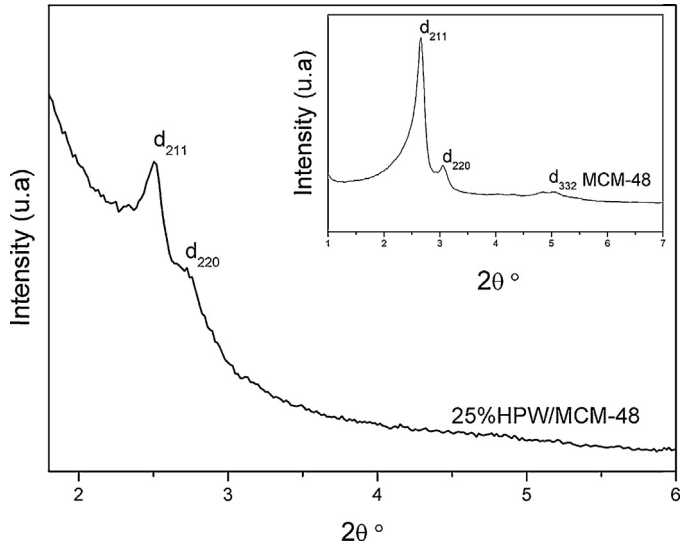


**Fig. 4.** XRD of MCM-48 and 25%HPW/MCM-48.

### 3.3. Surface area measurements

The total surface areas, the pore volumes, and pore size of all of the catalysts were calculated from the $N_2$ adsorption–desorption isotherms, and the results are summarized in Table 2.

Except for the 40%HPA/MK700, the surface area values of the 20–30%HPA/MK700 samples were greater than that of MK700. The pore volume of these samples decreased after the introduction of HPW, which was also observed by other researchers when using different supports for HPW loading [12,25]. With HPW loading percentages larger than 40%, the porous structure of MK700 begins to occlude or collapse; this conclusion was reached given that both surface area and pore volume drastically decreased for the 40%HPA/MK700 sample.

Both the surface area and pore volume of all of the molecular sieves decreased with HPW incorporation into MCM-41, MCM-48 and SBA-15. These results indicate that the HPW might be dispersed within the pore structure of these materials [4,11]. The nitrogen and XRD studies revealed that the incorporation of 25% HPW did not affect the mesoporous structures of these materials.

### 3.4. Fourier transform infrared spectroscopy (FT-IR)

The FT-IR spectra analyses of the supported samples were performed to investigate the presence of HPW on the catalyst surfaces. According to literature, HPW shows characteristic bands at 1080, 986, 888 and 820 $cm^{-1}$ that can be assigned to an asymmetric

**Table 2**
Physical properties of the samples.

| Sample | *SA* ($m^2$ $g^{-1}$)*Vp* ($cm^3$ $g^{-1}$)$D_A$ ($m^2$/g) | $V_p$ ($cm^3$/g) | $D_p$ (nm) |
|---|---|---|---|
| HPW | 0.37 | – | – |
| MK700 | 16.6 | 0.1 | – |
| 20%HPW/MK700 | 21.2 | 0.1 | – |
| 25%HPW/MK700 | 24.4 | 0.05 | – |
| 30%HPW/MK700 | 16.7 | 0.05 | – |
| 40%HPW/MK700 | 8.0 | 0.03 | – |
| MCM-41 | 1066 | 0.46 | 2.9 |
| 25%HPW/MCM-41 | 508 | 0.32 | 3.0 |
| MCM-48 | 992 | 0.57 | 5.4 |
| 25%HPW/MCM-48 | 487 | 0.59 | 4.5 |
| SBA-15 | 696 | 1.02 | 6.4 |
| 25%HPW/SBA-15 | 228 | 0.41 | 5.5 |

Surface area ($S_A$), pore volume ($V_P$) and pore diameter ($D_p$).

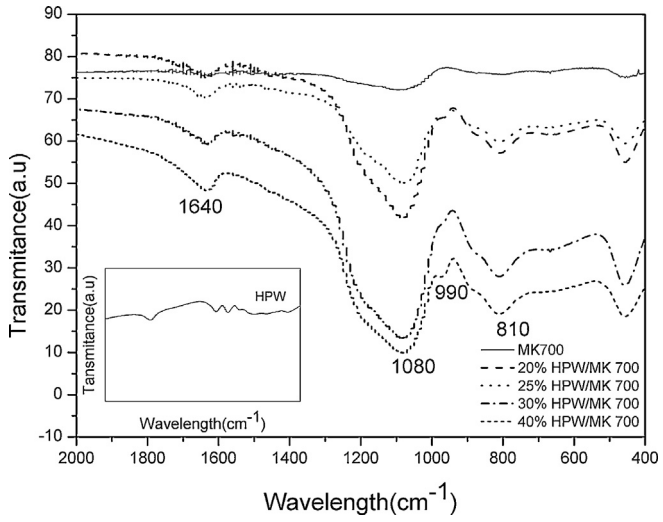


**Fig. 6.** FT-IR of MK700 and *x*%HPA/MK700.

stretching mode of the P–O, W = $O_t$, W–$O_c$–W, and W–$O_e$–W, where, t, c and e represent the specific positions (terminal, corner and edge-shared) of the different oxygen atoms in the Keggin structure observed for 12-tungstophosphoric acid [10,11,26,28].

Characteristic absorption bands of the Keggin anion from 700 to 1100 $cm^{-1}$ were observed in the samples with different amounts of HPW (see Figs. 6 and 7). The bands at 990 and 810 $cm^{-1}$ became more evident as the amount of HPW increased in the catalysts. This can be taken here as an evidence that the Keggin structure remains intact after the impregnation process. In addition to the characteristic band for HPW, FT-IR spectra of the samples also showed the infrared absorption peaks at 1640 $cm^{-1}$, probably corresponding to the bending and stretching vibrations of bridging hydroxyl groups because of the interaction of HPW anions and the surface silanol groups of the solids.

### 3.5. Surface acidity

The results of the theoretical and the actual number of surface protons of each support are presented in Table 3. A comparison between these values provided us information about the actual fraction of protons that were accessible by the used probe (KOH).

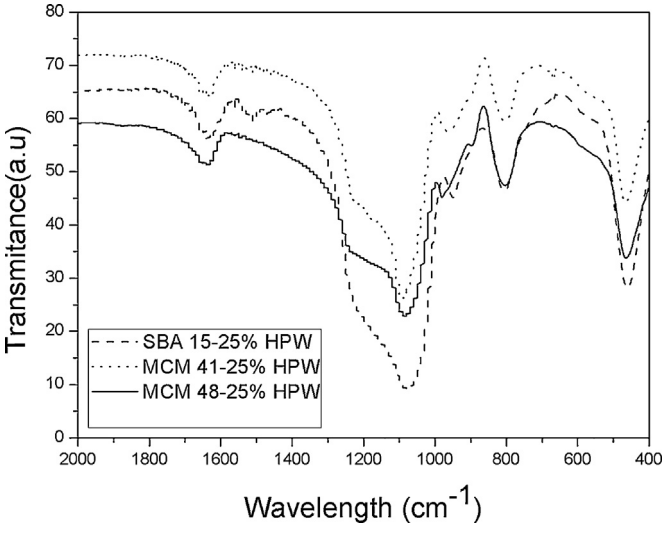


**Fig. 7.** FT-IR of 25%HPA modified mesoporous MCM-41, MCM-48 and SBA-15.

**Table 3**
Surface acidity of catalysts.

| Sample | Theoretical $H^+$ (mmol/$H^+$g)[a] | Actual $H^+$ (mmol/$H^+$g) |
|---|---|---|
| MK700 | 0 | 0 |
| 20%HPW/MK700 | 0.2083 | 0.20 |
| 25%HPW/MK700 | 0.2604 | 0.23 |
| 30%HPW/MK700 | 0.3125 | 0.25 |
| 40%HPW/MK700 | 0.4167 | 0.26 |
| MCM-41 | 0 | 0.25 |
| MCM-48 | 0 | 0.25 |
| SBA-15 | 0 | 0.25 |
| 25%HPW/MCM-41 | 0.2604 | 0.80 |
| 25%HPW/MCM-48 | 0.2604 | 0.80 |
| 25%HPW/SBA-15 | 0.2604 | 0.80 |

[a] Theoretical $H^+$ = [(%HPW/100) × 3/2880] × 1000.

As can be seen, the theoretical amount of protons in the 20%HPW/MK700 sample is 0.2083 mmol/g and the actual amount estimated was about 0.20 mmol/g. In this case, 96% of the protons were accessible by KOH. For 25%HPW/MK700 about 0.23 mmol $H^+$ react with KOH (88% of the total of 0.2604 mmol) and for 30%HPW/MK700 0.25 mmol $H^+$ react with KOH (80% of the total of 0.3125 mmol). With 40%HPW/MK700, the sample with the highest HPW content, about 0.26 mmol $H^+$ react with KOH (62% of the total of 0.4167 mmol). The results indicate that the access of the probe KOH on the active sites of the supported materials is achieved with lower HPW loadings.

Pure MCM-41, MCM-48 and SBA-15 surfaces have Si–OH (silanol groups) which are weakly acidic in nature. When these silanol groups were replaced the stronger acidic sites of HPW the number of surface acid sites increased in the supports.

### 3.6. Catalyst tests

Esterification reactions have low equilibrium constants and require the use of a catalyst to increase the reaction yield [8]. The conversion of fatty acids versus different amounts HPA supported on MK700 was evaluated at 130 °C for 1 h using a molar ratio of 1:10 DDPO: EtOH and 10 wt% catalyst (see Table 4). When the esterification reaction was performed without a catalyst, the fatty acids conversion was 18%. For MK700 (%HPA = 0), this conversion was only 19%, showing that the catalytic contribution of MK700 is negligible. The results show that the conversion rate increased as the HPW content increased on the MK700 support.

To evaluate whether the chemical reaction was in fact performed on the heterogeneous phase, we monitored the amount of tungsten on the catalyst before and after the chemical reactions by XRF analysis. The preliminary results revealed that, under the studied conditions, the catalytic process is heterogeneous but with a great contribution of a homogeneous phase related to the HPW leaching from MK700 (Table 4).

**Table 4**
Esterification of DDPO using EtOH versus different amounts of HPW/MK700 and the leaching of $WO_3$.

| Catalyst | $C_{FFA}$ (%) | $WO_3$ (wt%)[a] | $WO_3$ (wt%)[b] | $WO_3$ leaching (wt%) |
|---|---|---|---|---|
| No catalyst | 18 | 0 | 0 | – |
| MK700 | 19 | 0 | 0 | – |
| 20%HPW/MK700 | 26 | 19 | 14 | 26.3 |
| 25%HPW/MK700 | 55 | 24 | 14 | 41.6 |
| 30%HPW/MK700 | 57 | 30 | 17 | 43.3 |
| 40%HPW/MK700 | 72 | 40 | 21 | 32.5 |

Reaction conditions: 1 h, 130 °C, DDPO: EtOH molar ratio 1:10, 10 wt% of catalyst.
[a] $WO_3$ by XRF before the reaction.
[b] $WO_3$ by XRF after the reaction.

**Table 5**
Esterification of DDPO with EtOH versus time.

| Time (h) | $C_{FFA}$ (%) |
|---|---|
| 1 | 45 |
| 2 | 60 |
| 3 | 72 |
| 4 | 79 |

Reaction condition: 130 °C, 10 wt% of 25%HPW/MK700, molar ratio DDPO:EtOH 1:10.

HPW is very soluble in ethanol, and its leaching from the support depends on the catalyst preparation [10,11]. With this in mind, from that point on we have chosen the 25%HPA/MK700 sample to investigate the leaching processes in details.

To eliminate the excess of HPW from 25%HPA/MK700 sample that can be responsible for the homogeneous phase of the reaction, this solid was purified in a Soxhlet extractor with a mixture of $CH_2Cl_2$ and $(C_2H_5)_2O$ (50 mL each) for 24 h, washed with water, air-dried, and then analyzed by EDX. It was observed that 43.2% of the original HPW amount supported had been leached (see supplementary material). So, the actual HPW loading of the final catalyst was 14.2%. The purified 25%HPW/MK700 solid was then thermal activated at 130 °C before being used as a catalyst.

To evaluate the influence of time and temperature on the esterification of DDPO with ethanol the reaction was performed over purified 25%HPA/MK700 solid. Table 5 shows the obtained conversion values at 130 °C when the reaction time was varied from 1 to 4 h. As can be seen, the conversion rate increased from 45 to 60% in the first 2 h and then remains almost constant with further increase of reaction time more than 3 h.

The esterification of DDPO with ethanol (1:10) was then performed at the following different temperatures: 70, 85, 100, 130, 150, 170 and 200 °C using 10 wt% of purified 25%HPA/MK700 for 2 h (see Table 6). The conversion varied from 12.5% (70 °C) to 83% (200 °C). A significant increase in the overall yield is observed with increasing temperature until 150 °C after which a slight increase in the yield is observed. From 150 to 170 °C the yield reached a near saturation of conversion (70–72%), and at 200 °C the yield reached 83%. A possible explanation for this observation could be the water sorption on the active sites of the catalyst which yielded from esterification process, and/or increase of the reverse hydrolysis reaction rate. With the obtained results, it was possible to conclude that the increase in temperature was a crucial factor to increase the conversion of fatty acids. The temperature of 200 °C was considered as the optimum temperature for the esterification of DDPO.

Several reports in the literature establish first-order kinetics for esterification reaction [2,12,27]. To calculate the rate constants ($k$) for the esterification of DDPO over 25%HPW/MK700 catalyst we have adjusted the data for the first-order reaction and plotted −ln (1 − conversion) versus time for the following temperatures: 70, 85 and 100 °C (see Fig. 8). The obtained values were 0.00107 at 70 °C, 0.00122 at 85 °C and 0.00185 at 100 °C. The regression coefficients of the straight lines showed good fits to first-order kinetics. From the $k$ values, we plotted ln($k$) versus 1/temperature

**Table 6**
Esterification of DDPO with EtOH versus temperature.

| Temperature (°C) | $C_{FFA}$ (%) |
|---|---|
| 70 | 12.5 |
| 85 | 15.5 |
| 100 | 20.2 |
| 130 | 60.0 |
| 150 | 70.0 |
| 170 | 72.0 |
| 200 | 83.0 |

Reaction condition: 2 h, 10 wt% of 25%HPW/MK700, molar ratio DDPO: EtOH 1:10,

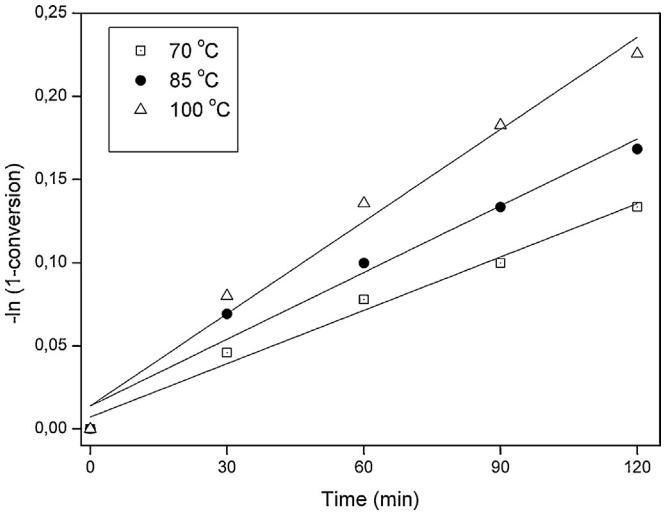


**Fig. 8.** Plots of −ln(1 − conversion) versus time at different temperatures.

(Fig. 9) and calculated the apparent activation energy (Ea), which was 19.78 kJ/mol. Low activation energy (10–15 kJ/mol) indicates that the process is diffusion controlled [4]. So, in the present case the activation energy was 19.78 kJ/mol and hence the chemical reaction was the rate controlling step.

The esterification of DDPO with ethanol was also performed over 25%HPW/MCM-41, 25%HPW/MCM-48 and 25%HPW/SBA-15 mesoporous samples. The 25%HPW/MCM-48 catalyst, which exhibited the lowest conversion value (75 wt%), showed equivalent to 0 wt% leaching. The 25%HPW/MCM-41 and 25%HPW/SBA-15 catalysts showed approximately 1.6 and 0.8 wt% leaching, respectively. These results suggest that the cubic pore structure of MCM-48 is more favorable to accommodate HPW than the unidirectional pore structure of MCM-41 and SBA-15.

Some authors admit that in the heterogeneous process the leaching of the active phase of a catalyst should not exceed 2.7 wt% [27]. So, from the $WO_3$ leaching results presented in Table 7 it was possible to conclude that the conversion of DDPO was driven by HPW in a predominantly heterogeneous phase when using MK700 and mesoporous materials as supports.

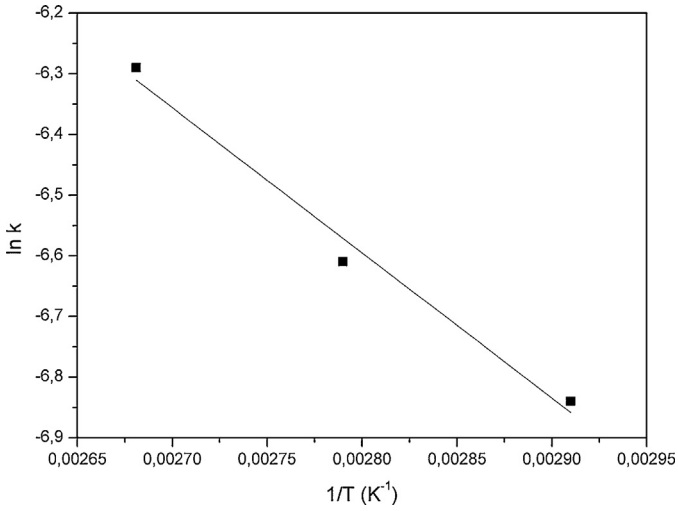


**Fig. 9.** Arrhenius plot of ln($k$) versus 1/$T$ for reaction of DDPO with ethanol.

**Table 7**
Esterification of DDPO with EtOH using different catalysts.

| Catalyst | $C_{FFA}$ (%) | $WO_3$ (wt%)[a] | $WO_3$ (wt%)[b] | $WO_3$ leaching (wt%) |
|---|---|---|---|---|
| 25% HPW/MK700 | 83 | 14.2 | 14.0 | 1.4 |
| 25% HPW/MCM-41 | 79 | 25.0 | 24.6 | 1.6 |
| 25% HPW/MCM-48 | 75 | 25.0 | 25.0 | 0.0 |
| 25% HPW/SBA-15 | 82 | 25.0 | 24.8 | 0.8 |

Reaction condition: 200 °C, molar ratio DDPO: EtOH 1:10, 10 wt% of catalyst.
[a] $WO_3$ by XRF before the reaction.
[b] $WO_3$ by XRF after the reaction.

### 3.7. Reuse of the spent catalyst

After the first use and before every reuse, the 25%HPW/MK700 catalyst was separated from the reaction media by filtration, washed with a mixture of $CH_3CH_2OH$ and $H_2O$ (100 mL each), dried at room temperature, and then activated at 130 °C before being used in the esterification of DDPO with ethanol. The reaction was performed at 200 °C for 2 h (1 mol DDPO: 10 mol ethanol and 10 wt% catalyst). The overall yield after the first reuse was 79%, i.e., 90% of the original value (83%). This could be probably caused by the loss of catalyst due to filtration and washing processes, since no leaching of HPW was observed. After the second and the third cycle, the overall yield drastically decreased to 45 and 20%, respectively, and a large amount of HPW was leached from the support. After the second cycle, only about 9.7% of HPW was left on the support, and after the third cycle, this amount was only about 5.5%. The recyclability results suggest that the catalyst can be reused with relatively stable activity just in the first cycle of reuse. Further work to improve stabilization is warranted.

## 4. Conclusion

The incorporation of HPW into kaolin waste (MK700), MCM-4, MCM-48 and SBA-15 has been described. The obtained solid acid catalysts were used in the esterification reaction of DDPO with ethanol. If the 25%HPW/MK700 catalysts is used in the reaction without a purification step, a great amount of HPW is leached and the reaction is not governed by heterogeneous mode. The amount of HPW that can be loaded into 25%HPW/MK700 after the prior purification procedure is 14.2%. The purified 25%HPW/MK700 is an active catalyst for the esterification of DDPO with ethanol reaching 83% conversion at 2 h reaction with 1:10 (DDPO:ethanol) molar ratio and. The results indicated that HPW supported on kaolin waste can provide significant advances in the development of environmentally benign processes in the chemical industry. It also can be concluded that the studied solids (MK700, MCM-4, MCM-48 and SBA-15) are promising supports for HPW and appear to be attractive heterogeneous catalysts for preparation of esters by the esterification of low-quality oils and fats.

## Acknowledgments

The authors would like to thank CAPES for a Doctoral scholarship to L.H.O.P, and FINEP/SIPI, FAPESPA/Vale and CNPq for the financial support.

## Appendix A. Supplementary data

Supplementary data associated with this article can be found, in the online version, at http://dx.doi.org/10.1016/j.apcatb.2014.04.039.

## References

[1] L.P.F.C. Galvão, M.N. Barbosa, A.S. Araujo, V.J.F Júnior, Quim. Nova 35 (2012) 41–44.
[2] L.A.S. Nascimento, R.S. Angélica, C.E.F. Costa, J.R. Zamian, G.N. Rocha Filho, Appl. Clay Sci. 51 (2011) 267–273.
[3] A.P.S. Dias, J. Bernardo, P. Felizardo, M.J.N. Correia, Energy 41 (2012) 344–353.
[4] V. Brahmkhatri, A. Patel, Appl. Catal., A: Gen. 403 (2011) 161–172.
[5] L.A.S. Nascimento, R.S. Angélica, C.E.F. da Costa, J.R. Zamian, G.N. Rocha Filho, Bioresour. Technol. 102 (17) (2011) 8314–8317.
[6] H. Liu, N. Xue, L. Peng, X. Guo, W. Ding, Y. Chen, Catal. Commun. 10 (2009) 1734–1737.
[7] J.L. Ropero-Veja, A. Aldana-Peres, R. Gómez, M.E. Niño-Gómez, Appl. Catal., A: Gen. 379 (2010) 24–29.
[8] J. Clayden, N., Greeves, S., Warren, P., Wothers, Organic Chemistry, 1st ed., Oxford University Press, 2000, pg 288.
[9] S. Wu, W. Zhang, J. Wang, X. Ren, Catal. Lett. 123 (2008) (2008) 276–281.
[10] E.V. Ramos-Fernandez, P. Pieters, B. Linden, J. Juan-Alcañiz, P. Serra-Crespo, M.W.G.M. Verhoeven, H. Niemantsverdriet, J. Gascon, F. Kapteijn, J. Catal. 289 (2012) 42–52.
[11] A.E.R.S. Khder, H.M.A. Hassan, M.S. El-Shall, Appl. Catal. A: Gen. 411–412 (2012) 77–86.
[12] C.F. Oliveira, L.M. Dezaneti, F.A.C. Garcia, J.L. Macedo, J.A. Dias, S.C.L. Dias, K.S.P. Alvim, Appl. Catal., A: Gen. 372 (2010) 153–161.
[13] V. Brahmkhatri, A. Patel, Appl. Catal., A: Gen. 403 (1–2) (2011) 161–172.
[14] Z. Yu, Y. Chen, Z. Shi, B. Zhao, Z. Zhao, C. Chen, P. Wan, Ind. Eng. Chem. Res. 50 (2011) 8524–8528.
[15] F.L. Linares, L. Carbognani, C.S. Stull, P.P. Almao, Energy Fuels 22 (2008) 2188–2194.
[16] B.S. Carneiro, R.S. Angélica, T. Scheller, E.A.S. de Castro, R.F. Neves, Cerâmica 49 (2003) 237–244.
[17] S.P. Da Paz, R.S. Angélica, R.F. Neves, Quím. Nova 33 (2010) 579–583.
[18] Q. Cai, W.Y. Lin, F.S. Xiao, W.Q. Pang, X.H. Chen, B.S. Zou, Microporous Mesoporous Mater. 32 (1999) 1–15.
[19] K. Schumacher, M. Grün, K.K. Unger, Microporous Mesoporous Mater. 27 (1999) 201–206.
[20] P. Yang, S. Huang, D. Kong, J. Lin, H. Fu, Inorg. Chem. 46 (2007) 203–321.
[21] D.S. Moraes, R.S. Angélica, C.E.F. Costa, G.N. Rocha Filho, J.R. Zamian, Appl. Clay Sci. 51 (2011) 209–213.
[22] N. Özbay, N. Oktar, N.A. Tapan, Fuel 87 (2008) 1789–1798.
[23] L.A.S. do Nascimento, L.M.Z. Tito, R.S. Angélica, C.E.F. da Costa, J.R. Zamian, G.N. da Rocha Filho, Appl. Catal., B: Environ. 101 (2011) 495–503.
[24] J. Wang, J. Lu, J. Yang, W. Xiao, Mater. Lett. 78 (2012) 199–201.
[25] E. Caliman, J.A. Dias, S.C.L. Dias, F.A.C. Garcia, J.L. de Macedo, L.S. Almeida, Microporous Mesoporous Mater. 132 (2010) 103–111.
[26] R. Neumann, M. Dahan, Polyhedron 6 (19) (1998) 2446–2453.
[27] O.S.J. Lacerda, R.M. Cavalcanti, T.M. Matos, R.S. Angélica, G.N. da Rocha Filho, I.C.L. Barros, Fuel 108 (2013) 604–611.
[28] K. Srilatha, R. Sree, B.L.A. Prabhavathi Devi, P.S. Sai Prasad, R.B.N. Prasad, N. Lingaiah, Bioresour. Technol. 116 (2012) 53–57.
[29] J.A. Dias, E. Caliman, S.C.L. Dias, Microporous Mesoporous Mater. 76 (2004) 221–232.
[30] J.A. Dias, J.P. Osegovic, R.S. Drago, J. Catal. 183 (1999) 83–90.